Available online at www.sciencedirect.com
SCIENCE DIRECT
Medical Engineering & Physics 27 (2005) 845–861
Medical Engineering & Physics
www.elsevier.com/locate/medengphy

Three-dimensional finite element modeling of ligaments: Technical aspects

Jeffrey A. Weiss [a,b,c,*], John C. Gardiner [a,1], Benjamin J. Ellis [a,c], Trevor J. Lujan [a,c], Nikhil S. Phatak [a,c]

[a] *Department of Bioengineering, University of Utah, 50 South Central Campus Drive, Room 2480, Salt Lake City, UT 84112, USA*
[b] *Department of Orthopedics, University of Utah, UT, USA*
[c] *Scientific Computing and Imaging Institute, University of Utah, UT, USA*

Received 11 October 2004; received in revised form 25 April 2005; accepted 21 May 2005

Abstract

The objective of this paper is to describe strategies for addressing technical aspects of the computational modeling of ligaments with the finite element (FE) method. Strategies for FE modeling of ligament mechanics are described, differentiating between whole-joint models and models of individual ligaments. Common approaches to obtain three-dimensional ligament geometry are reviewed, with an emphasis on techniques that rely on volumetric medical image data. Considerations for the three-dimensional constitutive modeling of ligaments are reviewed in the context of ligament composition and structure. A novel approach to apply in situ strain to FE models of ligaments is described, and test problems are presented that demonstrate the efficacy of the approach. Approaches for the verification and validation of ligament FE models are outlined. The paper concludes with a discussion of future research directions.

Keywords: Finite element; Ligament; Joint mechanics; Constitutive model; In situ strain; Subject-specific

1. Introduction

The skeletal ligaments are short bands of tough fibrous connective tissue that bind bones together across joints. Their mechanical function is to guide normal joint motion and restrict abnormal joint movement. These functions are assisted by the congruent geometry of the articulating joint surfaces and musculotendinous forces. Ligaments can be subjected to extreme stress while performing their role in restricting abnormal joint motions and can be damaged or completely disrupted when overloaded. Excessive stretching or disruption can result in gross joint instability, resulting in altered joint kinematics, altered load distribution, and increased vulnerability to injury of other ligaments and musculoskeletal tissues. Eventually, degenerative joint disease may result from alterations in load bearing and joint kinematics.

Because ligamentous instability can greatly restrict the activity level of an individual and may result in degenerative disease, basic and applied research efforts have examined ligament injury mechanisms, techniques for ligament repair and reconstruction, and rehabilitation methods for use during the healing period. These studies have helped to elucidate details of the natural history of ligament injury and healing from biomechanical, histological, and biochemical viewpoints. However, fundamental mechanical questions regarding the role of individual ligaments, the mechanisms of ligament injury, and the efficacy of reparative/reconstructive procedures persist. This is partially due to inherent limitations of experimental studies such as their high cost, low sensitivity, and the difficulties associated with accurate measurement of basic kinematic and mechanical quantities, both in vivo and in vitro. The use of computational methods for the study of joint mechanics can elucidate ligament function and yield information that is difficult or impossible to obtain experimentally

* Corresponding author. Tel.: +1 801 587 7833; fax: +1 801 585 5361.
E-mail address: jeff.weiss@utah.edu (J.A. Weiss).
[1] Present address: MEA Forensic Engineers and Scientists, Lake Forest, CA, USA.

1350-4533/$ – see front matter © 2005 Published by Elsevier Ltd on behalf of IPEM.
doi:10.1016/j.medengphy.2005.05.006

[2–6]. In particular, the finite element (FE) method offers the ability to predict spatial and temporal variations in stress, strain, and contact area/forces. The FE method also provides a standardized framework for parameter studies, such as evaluation of multiple clinical treatments. Further, subject-specific FE modeling of ligament stress–strain behavior can potentially accommodate the large intersubject variability in joint kinematics and resting ligament tensions, which can limit the sensitivity of experimental and clinical investigations [7].

The vast majority of studies that have employed computational methods to examine ligament mechanics have used a one-dimensional representation of ligament geometry [3,8–10]. This entails using either single- or multiple-line elements [10] while allowing load transfer to bones at single or multiple points [11]. A one-dimensional representation requires only a few parameters to control load-elongation behavior, and overall in situ tension can be specified with a single scalar value. This approach has proved useful for predicting joint kinematics under the application of external loads (e.g., [12]), but it possesses several significant shortcomings: (1) nonuniform, 3D stresses and strains cannot be predicted, and (2) multiple sets of parameters and initial tensions routinely produce nearly identical predictions of joint kinematics. Ligaments are subjected to highly nonuniform deformations in vivo that result from a combination of tension, shear, bending, and compression [13,14], and the regional contribution of a ligament to joint stability changes with joint orientation [15–20]. A three-dimensional FE modeling approach is required to capture these characteristics.

Three-dimensional FE modeling of ligament stress–strain behavior is complicated by highly anisotropic, nonlinear material behavior, large deformations and complex geometry and boundary conditions. The objectives of this paper are to describe strategies for addressing these important technical aspects of the computational modeling of ligaments with the FE method. In particular, this paper describes strategies for FE modeling of ligament mechanics, methods for obtaining ligament geometry for computational models, considerations for the constitutive modeling of ligaments, the representation of in situ strains in FE models of ligaments, and the verification and validation of ligament FE models. Focus is placed on techniques that can be used when representing ligaments with three-dimensional continuum or shell elements.

2. Strategies for representing ligaments in joint models

Two strategies have been used for the three-dimensional FE analysis of ligament mechanics. In the first approach, a model of the entire joint is constructed, including all supporting soft tissue structures [21,22]. The influence of arbitrary external loads and/or displacements on joint kinematics and ligament mechanics can then be studied. This approach can predict joint kinematics, ligament stresses, strains, insertion site forces and load transfer to the bones via contact. However, the sheer complexity of such models makes this approach difficult to implement and the resulting models are nearly impossible to validate without detailed experimental studies. In the second approach, a single ligament is represented in the FE model. The motion of the ligament insertion sites, or alternatively the bones to which it is attached, is prescribed based on experimental kinematic measurements [6,7,23–25]. This approach provides predictions of ligament stresses, strains, insertion site forces and load transfer to the bones via contact, but not joint kinematics, since the motion of the bones must be prescribed. FE models of this kind are considerably easier to implement and validate. Since the overall stiffness characteristics of joints from different donors/animals routinely differ by a factor of two or more, this approach generally requires subject-specific measurements of joint kinematics [7].

3. Ligament geometry for computational models

3.1. Geometry acquisition

The acquisition of accurate geometry for the ligament(s) and possibly the bones is a fundamental requirement for the construction of three-dimensional FE models of ligaments. Laser scanning and medical imaging are the primary techniques that have been used for this purpose. Laser scanning can be very accurate, but cannot differentiate between the ligament of interest and surrounding bone and soft tissue structures. Further, it can only digitize geometry that is visible directly from the laser source. Both magnetic resonance imaging (MRI) and computed tomography (CT) have been used to acquire ligament geometry [7,26]. MRI can provide detailed images of soft tissue structure in diarthrodial joints. It should be noted that standard clinical MRI pulse sequences do not result in images that have any substantial signal for ligament. Rather, the structure of ligament is defined by a lack of signal. This is primarily due to the rapid decay of signal intensity from collagen [11]. Reducing echo time (TE) below 2 ms is an important consideration for obtaining images of collagen-containing structures. Dual echo spoiled gradient (SPGR) pulse sequences (e.g., $TE_1 = \sim 1$ ms, $TE_2 = \sim 8$ ms) can be used to obtain MR signal from ligaments [27–29] (Fig. 1). However, these sequences are not commonly available in commercial scanner software at this time.

When compared to MRI, CT yields superior spatial resolution and a better signal-to-noise ratio. Further, CT provides excellent images of the bones around the joint, which often must be included in FE models of ligaments to represent ligament wrapping and insertion site geometry. Soft tissue is visible in standard CT images, but there is little difference in the signal between soft tissues, and thus, it can be difficult to distinguish the boundaries of a specific ligament in an intact joint (Fig. 1). For experiments on cadaveric tissue, this problem can be circumvented by performing a detailed dissection of the ligament before imaging. Even with such

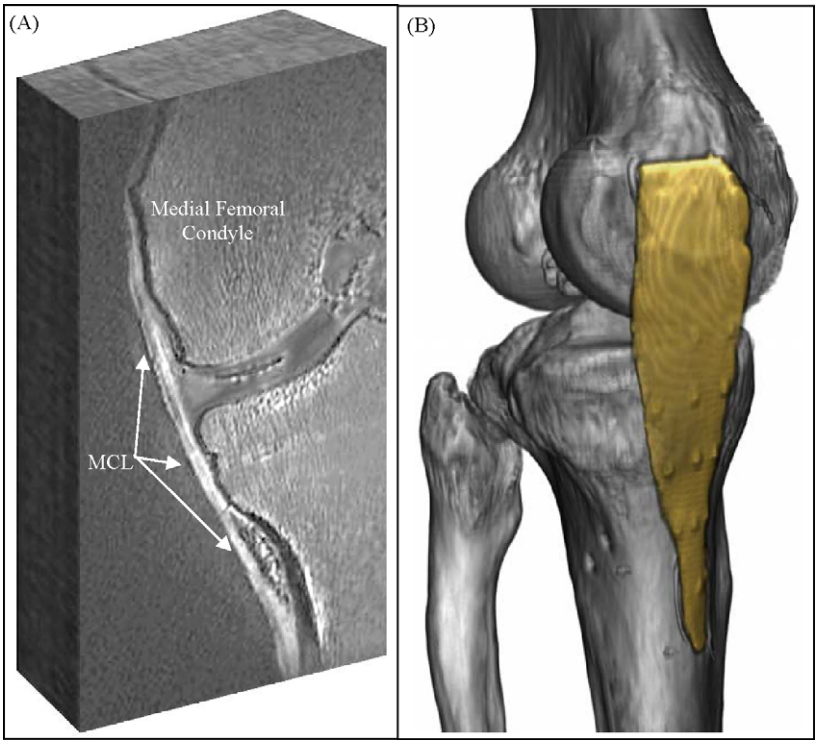

Fig. 1. Volumetric images of the human medial collateral ligament obtained from MRI (left) and CT (right). MR image geometry: Cropped to 180 × 340 (56 mm × 106 mm), 0.8 mm slice thickness; T2 processed dual echo image, TE1 = 1.63 ms, TE2 = 8.61 ms. CT image geometry: 512 × 512 acquisition matrix, 100 mm FOV, 1 mm slice thickness.

an approach, the exact location of the insertion sites can be difficult to determine, both with MRI and CT. To facilitate segmentation of ligaments and their insertions to bone in CT images, we use 30-gauge copper wire to mark the insertion sites before imaging (Fig. 2).

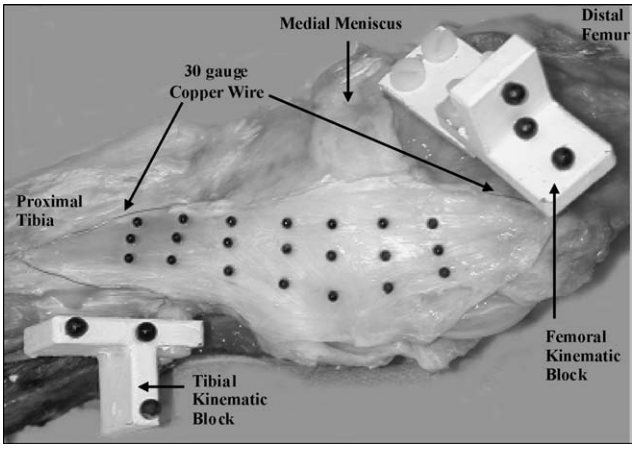

Fig. 2. Photograph of test setup for simultaneous measurement of MCL strain and knee joint kinematics. Twenty-one markers (2.38 mm dia.) were adhered to the MCL for strain measurement. Femoral and tibial kinematic blocks, each with three kinematic markers (4.75 mm diameter), were affixed to the cortical bone. The kinematic blocks provide a means to measure joint kinematics during experimental testing and to register the CT data with the configuration of the knee during experimental kinematic testing. Insertion sites were marked with 30 gauge copper wire.

It is often desirable to perform comparisons between FE predictions of joint kinematics or ligament strains and experimental measurements. Further, to drive FE models of individual ligaments as described above, one must be able to specify the initial relative orientation and position of bones to correspond with experimental measurements. The spatial configuration of the bones and/or ligaments that are obtained from medical image data must be registered with experimentally measured orientations. Since it is difficult to ensure that a joint is in the same position for medical imaging that it was during an experiment, fiducial markers must be placed on the bones before imaging [30]. Consideration should be given to the materials that are used to construct such fiducials so that they do not produce artifact in the image data. In our laboratory, we have used plastic markers attached to the bones with nylon screws (Fig. 2). The three-dimensional coordinates of the markers can be determined from segmentation of the image data, and their coordinates can be tracked during experiments using a motion analysis system [31].

3.2. Segmentation and geometry reconstruction

Extraction of the geometry of ligaments from CT or MRI data is performed by first segmenting the boundary of the structure. For in vitro studies using CT, this can be facilitated by marking the boundaries of the insertion sites with copper wire, as described above. Even with such an

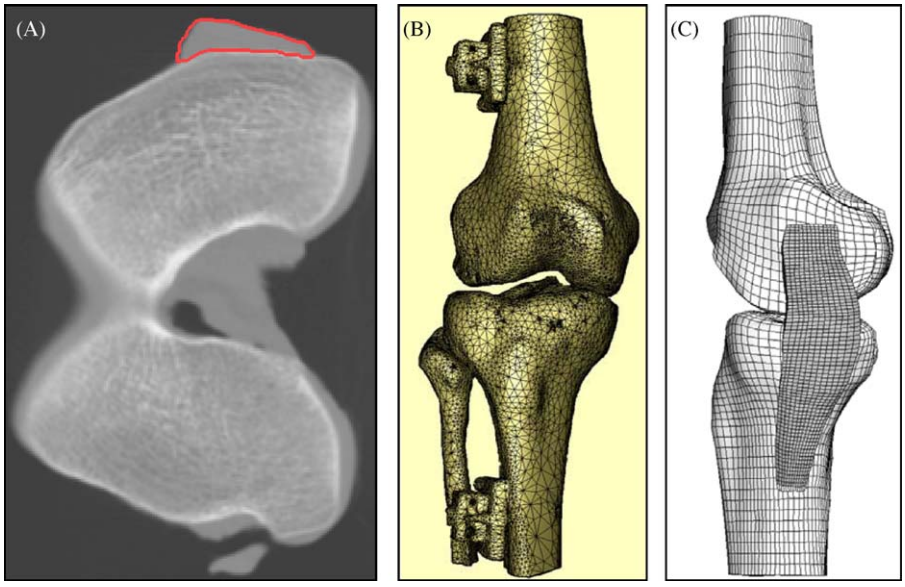

Fig. 3. (A) Single CT image slice through the distal femur showing manual segmentation of the MCL (red curve). Top of image is medial, left side of image is anterior. (B) Anterior view of isosurfaces of the femur and tibia extracted from the volumetric CT data using marching cubes. (C) Medial view of hexahedral FE meshes of the femur, MCL and tibia created from manually segmented contours of MCL and isosurfaces of femur and tibia.

approach, it is still generally necessary to perform manual (or semi-automatic) segmentation of ligament boundaries [6,7,23,32,33] (Fig. 3A). There are numerous software packages available for this purpose. We have obtained excellent results with the Surfdriver (www.surfdriver.com) and Amira (www.amiravis.com) software packages. Once the ligament of interest is segmented in the 3D image dataset, polygonal surfaces may be generated by either lacing together stacks of closed bounded contours [34] or by performing isosurface extraction on a binarized version of the segmented image dataset (Fig. 3B). If only the exterior geometry of the bones is needed (to model contact and wrapping of ligaments with bony surfaces), automatic segmentation via isosurface extraction can be performed with CT data. In our own research, we have used the marching cubes algorithm [35] to extract polygonal surfaces for the femur and tibia [7]. This technique produces a polygonal surface with an extremely large number of triangles, but reduction of the number of triangles can be achieved by using a decimation algorithm (e.g, [36]).

3.3. FE mesh generation

FE analysis of ligaments demands the use of element formulations that are accurate and robust for finite deformations. Historically, this has mandated the use of hexahedral elements. Many commercial software packages for FE mesh generation accommodate the generation of hexahedral meshes using mapping approaches. In our own research, we have used TrueGrid (XYZ Scientific Applications, Livermore, CA). The geometries of bones and ligaments are imported into the software as polygonal surfaces. If the bones are to be modeled as rigid bodies (an assumption that facilitates the application of experimentally measured kinematics to drive the motion of the bones), the polygons that represent the bone surfaces may be used directly to define the bone surfaces using rigid triangular shell elements [37]. FE meshes for the ligaments are constructed using a standard mapped meshing approach (Fig. 3C).

Formulations for tetrahedral elements that are accurate for finite deformations have been reported recently [38,39]. As these elements become widely available, mesh generation for ligaments may be greatly simplified by direct meshing of the closed polygonal surfaces with tetrahedrons.

Although hexahedral and tetrahedral elements are appropriate to discretize many ligaments, some ligaments are very thin, and thus, an inordinately large number of solid elements are needed to maintain reasonable element aspect ratios. Further, lower-order hexahedral elements tend to provide too stiff a response in bending for thin structures. An alternative approach is the use of shell elements. There are several shell element formulations that are valid for finite deformations (e.g., [40,41]). Shells have the advantage of providing more accurate simulation of bending behavior for thin structures (most brick element formulations are too stiff in bending). Mesh generation is considerably easier with shell elements than with solid elements and thickness may be assigned pointwise to shell elements. Further, they reduce the overall number of degrees of freedom in the system of equations. As an example, we have used shell elements to model the inferior glenohumeral ligament (IGHL) of the shoulder under anterior loading of the humerus [42] (Fig. 4A). Shell elements can represent the extensive folding that occurs in many capsular ligaments, such as the IGHL (Fig. 4B).

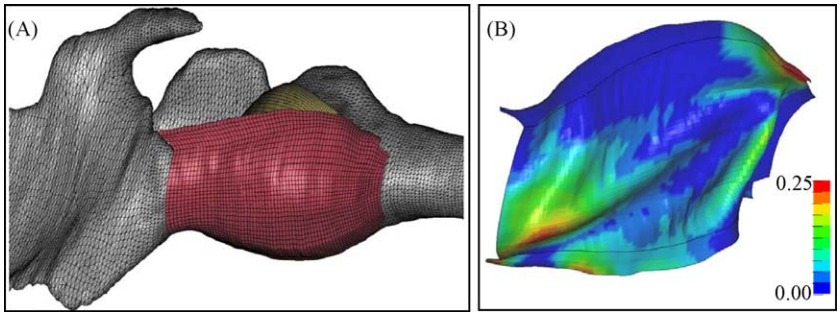

Fig. 4. Illustration of the use of shell elements for FE modeling of ligaments: (A) inferior view of an FE mesh of the inferior glenohumeral ligament of the shoulder, constructed from CT data. Scapula (left) and humerus (right) are shown in grey, IGHL (center) is shown in red, and cartilage is shown in yellow. Bone surfaces were imported directly into the FE preprocessing software and modeled as rigid triangular shells. The IGHL was represented with quadrilateral shell elements, and the cartilage was represented with hexahedral elements. Contact surfaces were defined between the IGHL and both the bones and cartilage. (B) 1st principal strain in the IGHL due to anterior translation of the humerus with respect to the scapula. The FE model was driven by experimentally measured kinematics of the bones during application of anterior loading by an orthopedic surgeon.

4. Constitutive modeling of ligaments

4.1. General considerations

Constitutive equations are used to describe the mechanical behavior of ideal materials through specification of the dependence of stress on variables, such as the deformation gradient, rate of deformation, temperature, and pressure. The accurate description and prediction of the three-dimensional mechanical behavior of ligaments by constitutive equations remains one of the challenges for computational modeling. The development and application of these constitutive models relies on an understanding of ligament structure and function, and knowledge of available experimental data. This section focuses on three-dimensional constitutive models for ligaments.

4.2. Structure and function of ligaments

Ligaments are highly anisotropic due to their fibrous structure. The degree of anisotropy can vary substantially between different types of ligaments [43–45] and the fiber orientation generally represents an adaptation to the mechanical environment. For instance, the collagen fibers in the cruciate ligaments of the knee are highly aligned with the long axis, while the organization of the inferior glenohumeral ligament of the shoulder varies considerably with location [46]. Collagen provides the primary resistance to tensile loading but offers negligible resistance to compression. Ligaments offer little resistance to bending, as illustrated by the fact that they will fold under their own weight when held vertically from the bottom.

All ligaments possess a toe region (an upwardly concave region) in the stress–strain curve for uniaxial loading along the predominant fiber direction [44,47–52]. The disappearance of this toe region is associated with the extinguishing of the crimp pattern in collagen fibers that can be viewed with polarized light [53]. Two approaches have been used in constitutive models to represent the origins of the toe region. The first approach uses numerous linear or bilinear elastic elements that are sequentially recruited to yield the nonlinear shape of the toe region. The second approach assumes that the toe region arises due to the wavy geometry of the collagen fibers.

A simplified explanation for the upwardly concave stress–strain behavior of ligaments was proposed by Viidik and Ekholm [53] and subsequently presented in more detail by Frisen et al. [54,55]. The elastic response of ligaments was represented by numerous individual linearly elastic components, each of which represented a collagen fibril of different initial length in its unloaded and crimped form. As the ligament was loaded, additional fibrils were recruited yielding the nonlinear behavior characteristic of the toe region. At higher loads, all the fibrils were loaded and the ligament stress–strain curve became linear. This approach provides a compact description of the uniaxial response of ligaments. Many subsequent models have used a similar assumption [48,49,56–64].

Others have represented the toe region as arising from the inherent crimp in collagen fibers. Diamant et al. [49] proposed a microstructural model for ligaments and tendons that represented the collagen crimp structure with straight elastic segments joined by rigid hinges. A similar structural model was developed for human patellar tendons by Stouffer et al. [65]. The collagen crimp pattern was represented by a kinematic chain composed of short elements connected by pins and torsion springs. A light microscope system was used to measure crimp pattern at different positions and under different loads to quantify model parameters. Individual link parameters were defined as functions of position to account for variations in crimp pattern. Comninou and Yannas [48] used a sinusoidal waveform to model the collagen crimp structure. Constitutive equations for uniaxial extension were formulated for a single fiber, as well as for a bundle of fibers embedded in a matrix. A constant crimp configuration was assumed that restricted this model to small strains. Lanir [57,62] also proposed a structural model for biological soft tissues that directly modeled the collagen fibrils.

Our laboratory examined changes in crimp period with applied tensile strain in rat tail tendons [50]. Results clearly demonstrated that the complete disappearance of crimp coincided with the end of the toe region. However, results also showed that the disappearance of crimp was not simultaneous in different regions of the tendon. Taken together, these observations support the hypothesis that the wavy, crimped geometry of the collagen fibril results in the nonlinearity in the toe region of the stress–strain curve in ligaments and tendons, but that the change in length of individual fibrils is spatially nonuniform with increasing tensile strain.

Ligaments have time- and history-dependent viscoelastic properties that arise from the interaction of water with the ground substance matrix and the inherent viscoelasticity of the solid phase. There have been numerous experimental investigations of the viscoelastic nature of ligaments (e.g., [51,66–74]). The loading and unloading curves of ligaments under tension do not follow the same path. Rather, a hysteresis loop is observed during cyclic tensile testing due to internal energy loss. Creep, an increase in deformation over time under a constant load, and stress relaxation, a reduction in stress over time under a constant deformation can both be observed in ligaments [66]. The effects of conditions, such as temperature [71] and hydration level [69] on the viscoelastic behavior of ligaments, has also been investigated. The variation of ligament stress–strain behavior with strain rate is another indicator of the viscoelastic nature of the tissue. Woo et al. [75] compared the material properties of rabbit medial collateral ligaments (MCLs) tested at five different strain rates. Results showed that changes in strain rate of over four orders of magnitude had relatively small effects on ligament material properties. Tensile strength and ultimate strain increased slightly with increasing strain rate while tangent modulus remained essentially unchanged. We recently reported the strain- and frequency-dependent viscoelastic behavior of the human MCL in tension along its longitudinal and transverse directions, and under shear along the fiber direction [74]. The results of this study support the conclusions of previous studies regarding small but significant increases in the effective modulus/dynamic stiffness of ligaments with increasing rate of loading.

Although often assumed to be incompressible due to their high water content, experimental evidence suggests ligaments undergo some volume change during deformations [76]. This volume change may occur due to fluid exudation [77,78] or as a result of inherent compressibility of the solid phase. Due to the limited availability of experimental data describing interstitial fluid flow in ligaments and tendons, FE models have been used to gain a better understanding of the flow behavior [79,80]. Chen et al. [80] created a microstructural model to study interstitial flow parallel and transverse to the collagen fibril direction, based on previously measured values for fibril diameter and water content. Results indicated that ligaments are likely to be much more permeable to flow in the longitudinal direction than in the transverse direction. Experiments in our laboratory on human MCL demonstrated that permeability transverse to the collagen fiber direction is slightly less than values reported for bovine articular cartilage, while at strains of 30% permeability was two to three times lower than that of bovine articular cartilage [77,81]. The contribution of fluid flow to the viscoelastic properties of ligaments is an area where further research is needed.

The material surrounding the collagen in ligaments is often referred to as the “ground substance”. It is composed of proteoglycans (PGs), glycolipids and fibroblasts and holds large amounts of water [82]. Proteoglycans consist of a protein core and one or more glycosaminoglycan side chains. Some proteoglycans aggregate with hyaluronic acid to form hydrophilic molecules. This interaction is responsible in part for the large amount of bound and unbound water in ligament: water typically comprises 60 to 70% of the total weight of normal ligaments [78,83,84].

Ligaments contain predominantly the small leucine-rich proteoglycans (SLRPs), such as the proteodermatan sulphates (e.g., decorin, biglycan) and proteokeratan sulphates of molecular mass ∼100 kDA. Approximately 50% of their mass is protein, with the rest being anionic glycosaminoglycans (aGAGs). In normal ligaments, decorin is the most abundant proteoglycan, accounting for about 80% [85]. The remainder is composed of biglycan, fibromodulin, versican and aggrecan. All of these proteoglycans are expressed in normal and healing ligaments [86]. Decorin carries a single dermatan sulphate side chain, while biglycan binds two chains of dermatan sulphate or chondroitin sulphate [87–89]. Decorin binds to type I collagen, while biglycan shows no affinity [90,91]. The glycan tails form antiparallel aggregates between their protein carriers, which are attached to collagen fibrils at binding sites occurring regularly along the fibril [88,90–93].

The main functions that have been attributed to proteoglycans are regulation of fibril growth and mechanical strengthening of the overall ligament or tendon. These proposed functions are primarily based on the analysis of tissues from mice that possess a targeted disruption in the decorin gene [94–99]. Studies of tendons during development have shown that PG content is inversely proportional to fibril diameter [89]. Graham demonstrated that PGs inhibit side-to-side fusion of collagen fibrils [100]. The mechanical function of proteoglycan-based fibril–fibril crosslinks is less clear. Proteoglycan deficiency does not alter the elastic uniaxial tensile mechanical properties of tendon (ultimate load, tensile strength, stiffness or modulus) when tested along the predominant fiber direction [94,101]. The elastic properties of decorin-deficient tendons when tested along their fiber direction appear to be unaffected [94]. Additional research is needed to elucidate the contribution of proteoglycans to ligament material properties, and thus provide a basis for improved constitutive models to study normal, injured and diseased ligaments.

4.3. Three-dimensional elastic constitutive models

As described earlier, the material behavior of ligaments is relatively insensitive to strain rate over several decades of variation. In addition, these tissues reach a "preconditioned" state following cyclic loading, after which there is a minimal amount of hysteresis. This has prompted many investigators to develop three-dimensional constitutive models that represent ligaments as nonlinear elastic. Beskos and Jenkins [102] proposed a continuum model that represented tendon as a fiber-reinforced composite. Inextensible fibers were arranged in a helical pattern and were embedded in an incompressible, hollow right circular cylinder. Ault and Hoffmann [103,104] developed a three-dimensional constitutive law for soft connective tissues that used a linearly elastic, composite materials approach. Lanir [64] used a strain energy approach to form a continuum model for fibrous connective tissue. The model described an incompressible composite of undulating collagen fibers embedded in a fluid matrix. The model assumed that the collagen fibers buckle under a compressive load and the unfolding of the fibers during deformation squeezed the matrix, resulting in an internal hydrostatic pressure. Hurschler et al. [105] proposed a three-dimensional model for tendon and ligament that included both micro structural and tissue level aspects. Similar to the approach of Lanir [64], it was assumed that the fibrils contributed to strain energy only when in tension, and the only contribution of the matrix was a hydrostatic pressure. A probability distribution function was used to describe the initial orientation of the collagen fibers in the tissue.

Our laboratory developed a structurally motivated continuum model to represent ligaments and tendons as nearly incompressible, transversely isotropic, hyperelastic materials [106–108]. The formulation used an uncoupled strain energy approach that allowed for a relatively straightforward FE implementation of the model. The model formulation also allowed for easy determination of matrix and fiber family material coefficients from experimental testing [44]. The model assumed that ligaments are locally transversely isotropic as a result of a single family of collagen fibers, and these fibers resist elongation and may interact with each other and the matrix [107,108]. The constitutive model was applied successfully to describe and predict three-dimensional strains in the human medial collateral ligament using subject-specific FE models [7]. This constitutive model has been adopted by other investigators [6,32] to describe the material behavior of the anterior cruciate ligament in the context of FE simulations.

4.4. Three-dimensional viscoelastic constitutive models

Although the effective modulus of ligaments is relatively insensitive to strain rate [74,108,109], viscoelasticity may be important when studying the response of joints to high-rate loading or impact scenarios [110]. In these situations, the rate of loading experienced by ligaments may vary dramatically between different locations within the tissue. Viscoelastic effects are also important when considering cyclic loading [74,111], creep, stress relaxation [108,112], or when studying tissue pathologies that alter viscoelastic behavior [113–117].

The time- and history-dependent behavior of ligaments has been the topic of many experimental studies of ligaments, and viscoelasticity has been incorporated into several three-dimensional constitutive models for ligaments. Lanir [118] extended his structural elastic model to incorporate three-dimensional viscoelasticity theory [119]. Viscoelasticity was similarly added to the structural model of Decraemer et al. [120] by assuming internal friction between fibers, and between fibers and the surrounding matrix. The damping was introduced by assigning linear viscoelastic properties to the fibers with a relaxation function. Sanjeevi et al. [121,122] described the viscoelastic behavior of biological soft tissues with an equation similar to that of a Voigt-type spring and dashpot model. Dehoff [123] and Bingham and Dehoff [124] modified a continuum-based constitutive equation that had been used to characterize the nonlinear viscoelasticity of polymers to describe the behavior of soft biological tissues. Ligaments were modeled as isotropic viscoelastic with fading memory.

Recent studies have based ligament viscoelasticity on nonlinear theories. Johnson's [125] single integral finite strain (SIFS) model describes finite deformation of a nonlinearly viscoelastic material within the context of a three-dimensional model. The specific form describing uniaxial extension was obtained, and the idea of conversion from one material to another (at a microscopic level) was then introduced to model the nonlinear behavior of ligaments and tendons. Pioletti et al. [126] introduced a framework based on elastic and viscous potentials. The resulting constitutive law is valid for large deformations and satisfies the principles of thermodynamics. Quaglini et al. [127] combined an anisotropic strain energy function and a discrete time black-box dynamic model, borrowed from the theory of system identification, to describe the time-dependent behavior of soft tissues. Bischoff et al. [128] developed a rheological network model using an orthotropic hyperelastic constitutive model for fibrous tissue and a viscoelastic reptation model for soft materials. Although a number of three-dimensional theories for nonlinear ligament viscoelasticity have been developed, there is still a need for experimental studies on ligament viscoelasticity that can provide the material coefficients that are necessary for anisotropic viscoelastic constitutive models.

4.5. Material coefficients for subject-specific modeling of ligaments

The use of anisotropic and/or viscoelastic constitutive models to describe the material behavior of ligaments requires the specification of a potentially large number of material coefficients. Complete data for these material coefficients are not available in the literature. In the context of anisotropic constitutive models, the material coefficients

cannot be obtained from a single material test configuration (e.g., a uniaxial tensile test) [44,128,129]. Similar problems exist for viscoelastic models, which may also be anisotropic in the elastic response or the viscoelastic response [51,128–131]. For in vitro studies, it is possible to perform multiple material tests on individual ligaments to obtain material coefficients for subject-specific modeling of ligament mechanics with anisotropic elastic consitutive models [7]. This approach is clearly not possible for models based on in vivo image data. Our laboratory has demonstrated that population-average material coefficients can provide reasonable predictions of strain in subject-specific FE models of the medial collateral ligament in the human knee [7]. However, this approach has yet to be evaluated for predictions of stress and insertion site forces.

5. In situ strain

When a ligament is separated from one or both of its insertions to bone, it will retract. The strain distribution that corresponds to that tension will be referred to herein as the in situ strain [19,132]. This terminology is used to differentiate it from residual strain/stress, which results from internal forces that are self-equilibrated without any externally applied boundary conditions. In the ligaments of diarthrodial joints, typical in situ strains are approximately 3–10% [17,19], and there is not a joint configuration in which the in situ strain is homogeneous. The resulting forces that are transmitted to the ligament insertion sites provide joint stability even in relatively neutral joint configurations [17,19]. The absence of these forces would result in a less stable joint, a condition that would be exacerbated by the upwardly concave tensile stress–strain behavior of ligaments. Failure to include in situ strain in FE models of ligaments can lead to large errors in subsequent calculations of stress and insertion site forces [25].

The experimental measurement of in situ strain is challenging. Typically, contrast markers are attached to the ligament and the spatial positions of the markers are recorded before and after separating the ligament from its insertions to bone [132]. This measurement provides information about the in situ strains on the surface of the ligament. We have developed a method to apply this in situ strain distribution to FE models of ligaments. The development extends our previous method [133] to allow the exact enforcement of experimentally measured in situ strains.

5.1. Multiplicative decomposition of deformation gradient

Three configurations are introduced—the stress-free state (0), the in situ strain state (R), and the current, deformed state (r) (Fig. 5). The multiplicative decomposition of the total deformation gradient, $\boldsymbol{F}_{0\to r}$ yields:

$$\boldsymbol{F}_{0\to r} = \boldsymbol{F}_{R\to r}\boldsymbol{F}_{0\to R} \tag{1}$$

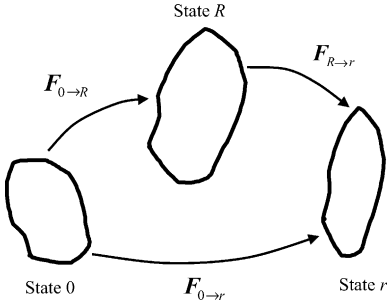

Fig. 5. Schematic of kinematic configurations used to describe the total deformation gradient $\boldsymbol{F}_{0\to r}$ as a multiplicative decomposition. State "0" indicates the stress-free reference configuration, state "R" indicates the configuration after in situ strain has been applied, and State "r" is the configuration after nonlinear FE equilibrium iterations achieve a minimum-energy configuration.

Here $\boldsymbol{F}_{0\to R}$ represents the deformation gradient due to the in situ strains and $\boldsymbol{F}_{R\to r}$ is the deformation gradient that results from subsequently applied loads.

To apply Eq. (1) directly, all nine components of the deformation gradient due to in situ strain, $\boldsymbol{F}_{0\to R}$, must be measured at every location in the ligament. It is much easier to measure the local fiber stretch λ_{exp} from contrast markers that have been distributed along the local fiber direction, $\boldsymbol{a}_0$. Further, direct application of Eq. (1) requires that the stress-free geometry of the ligament is available. As noted in Section 3 above, it is much easier to obtain the geometry of the ligament directly from medical image data in the configuration R. With these constraints on the available data, the challenge is to apply an experimentally measured in situ strain distribution to an FE model that was generated using geometry from configuration R.

The fiber stretch that corresponds to the total deformation gradient $\boldsymbol{F}_{0\to r}$ is defined as $\lambda_{0\to r}$. Similarly, the fiber stretches corresponding to $\boldsymbol{F}_{R\to r}$ and $\boldsymbol{F}_{0\to R}$ are defined as $\lambda_{R\to r}$ and $\lambda_{0\to r}$, respectively. With these definitions, Eq. (1) implies:

$$\lambda_{0\to r} = \lambda_{R\to r}\lambda_{0\to R} \tag{2}$$

5.2. Iterative update procedure

In situ strain is introduced in the FE formulation by specifying $\boldsymbol{F}_{R\to 0}$ at each integration point. During the nonlinear FE analysis, minimization of total system energy will determine a $\boldsymbol{F}_{R\to r}$ that balances the externally applied forces, boundary conditions, and internal stresses. As a result, in general $\boldsymbol{F}_{0\to r}$ will not equal $\boldsymbol{F}_{0\to R}$ and the total fiber stretch $\lambda_{0\to r}$ will not equal the experimentally measured fiber stretch λ_{exp}. This is especially problematic for ligament geometries that demonstrate curvature and variation in cross-section along their length, and for applying in situ strain distributions that are inhomogeneous. Thus, the objective is to enforce the constraint $\lambda_{0\to r} = \lambda_{\text{exp}}$ before applying any additional forces/displacements to the ligament FE model.

As an initial estimate, $\boldsymbol{F}_{0\to R}$ was assumed to consist of a uniaxial stretch $\lambda_{0\to R}$ along the fiber direction in a local coordinate system aligned with the fiber direction. The deformation gradient due to in situ strains in a coordinate system with the "11" direction aligned with the local fiber direction is then:

$$[\overline{\boldsymbol{F}}_{0\to R}] = \begin{bmatrix} \lambda_{0\to R} & 0 & 0 \\ 0 & 1 & 0 \\ 0 & 0 & 1 \end{bmatrix}. \tag{3}$$

This tensor is transformed to the global coordinate system for computation of $\boldsymbol{F}_{0\to r}$:

$$\boldsymbol{F}_{0\to R} = \boldsymbol{Q}\overline{\boldsymbol{F}}_{0\to R}, \tag{4}$$

where $\boldsymbol{Q}$ is a rotation between the fiber coordinate system and the global coordinate system.

An iterative update procedure was implemented to enforce the constraint $\lambda_{0\to r} = \lambda_{\text{exp}}$. Using Eq. (2), this constraint can be rewritten as:

$$\lambda_{R\to r}\lambda_{0\to R} = \lambda_{\text{exp}}. \tag{5}$$

Since $\lambda_{R\to r}$ is determined by the minimization of energy in the nonlinear FE program, Eq. (5) is rewritten as a constraint on $\lambda_{0\to R}$:

$$\lambda_{0\to R} = \frac{\lambda_{\text{exp}}}{\lambda_{R\to r}}. \tag{6}$$

Eq. (6) was enforced using an augmented Lagrangian iterative update of $\lambda_{0\to R}$ [134,135] at the integration points:

Initialize $\lambda^0_{0\to R} = \lambda_{\text{exp}}$
$k = 0$
DO for each augmentation k WHILE $\left\|\left(\lambda^{k+1}_{0\to R} - \lambda^{k}_{0\to R}\right)/\lambda^{k}_{0\to R}\right\| > \text{TOL}$
    Minimize potential energy with $\lambda^{k}_{0\to R}$ fixed using quasi-Newton method [1]
    Calculate error: $\alpha^{k+1} = \lambda_{\text{exp}}/\lambda^{k}_{R\to r} - \lambda^{k}_{0\to R}$
    Update Lagrange Multipliers: $\lambda^{k+1}_{0\to R} = \lambda^{k}_{0\to R} + \alpha^{k+1}$
END DO

This iteration procedure is referred to as the Uzawa algorithm [136,137]. The constraint in Eq. (6) can be satisfied to a user-defined tolerance (usually TOL = 0.05, implying that the multipliers changes by less than 5% between augmentations).

This approach is not limited to any particular constitutive model for the ligament, although in practice the direction $\boldsymbol{a}_0$ is selected to correspond to the local fiber direction in a transversely isotropic hyperelastic constitutive model.

5.3. Test problem-curvature

As mentioned previously, the curvature associated with many ligaments as they wrap around bones is one of the sources of problems when applying in situ strains to FE models of ligaments. In this test problem, the objective was to apply a uniform fiber strain of 3% along the curved axis of an FE mesh that was fully constrained on both ends (Fig. 6A and B). Three-field hexahedral elements were used [107] and material coefficients and constitutive model were based on our previous study [7]. Without augmentations, the attempt to apply a uniform strain fails miserably, as the freedom of elements to move during the equilibrium iterations results in a highly nonuniform strain distribution that is much lower than the target value of 3% (Fig. 6C). With augmentations, the fiber strain distribution converges quickly to the desired homogenous distribution (Fig. 6D–F).

5.4. Test problem—femur–medial collateral ligament–tibia complex

This problem demonstrates the effectiveness of the augmented Lagrangian technique in a three-dimensional model of the MCL that includes nonuniform ligament cross-section, curvature as the MCL wraps around the tibia and a highly inhomogeneous in situ strain distribution. A subject-specific FE model of the human femur–MCL–tibia complex was constructed [7]. For this same knee, the in situ strain distribution was measured experimentally at 0 degrees of knee flexion, and the material coefficients for the transversely isotropic constitutive model were based on experimental material testing of the MCL [44,108]. Experimental in situ strain data ($\lambda_{\text{exp}} - 1$) were interpolated over the FE mesh to provide a smooth, continuous distribution (Fig. 7, left panel). The in situ strain distribution was then applied to the MCL using Eq. (1) without augmentations. Contact and load transfer between the MCL and bones was accommodated using the penalty method [138].

Using the standard procedure without augmentation yields a total in situ fiber strain ($\lambda_{0\to r} - 1$) that is much lower and less inhomogeneous than the target in situ strain distribution (compare left and middle panels of Fig. 7). In contrast, a TOL of 0.05 was achieved with six augmentations using the algorithm described above, and the resulting in situ strain distribution is nearly identical to the experimental distribution (compare left and right panels of Fig. 7). The small differences between these two images are the result of using nodal values for interpolation in the left panel and enforcing the constraint at the integration points in the right panel.

5.5. Alternative approaches

Even greater complications arise when one wishes to consider in vivo studies of ligament mechanics on a patient-specific basis. With a database of in situ strain values for

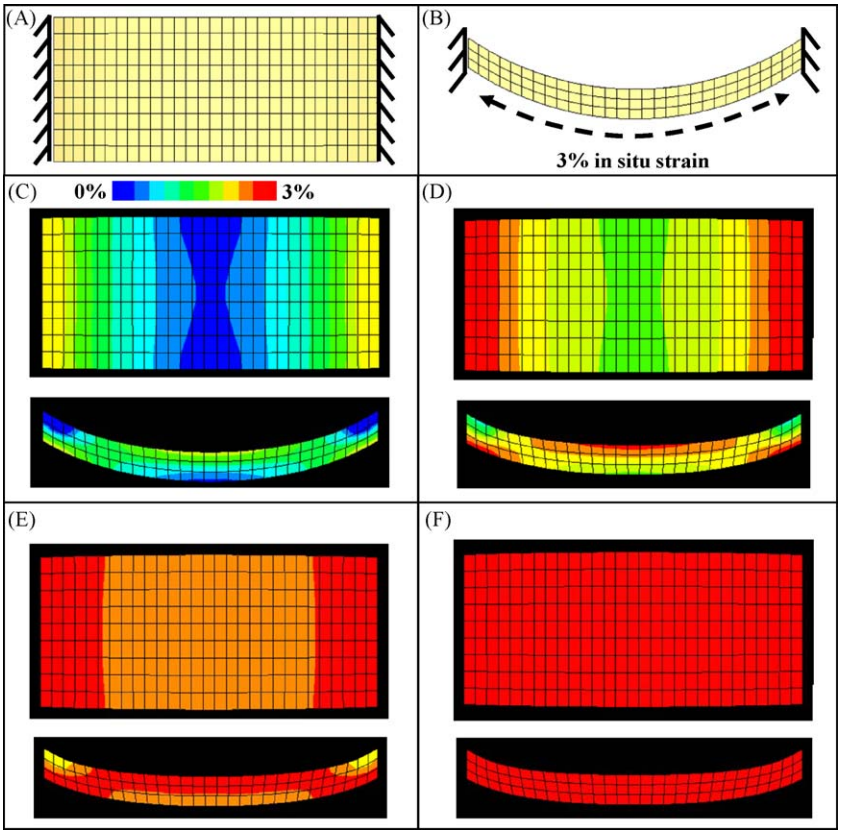

Fig. 6. Test problem of a curved test sample to demonstrate performance of the iterative update procedure to enforce in situ fiber strain. The objective is to achieve an in situ fiber tensile strain of 3%. (A) Top view of FE mesh. Nodes at both ends are fully constrained. The local fiber direction is oriented from left-to-right. (B) Side view of the same FE mesh. The local fiber direction follows the curvature of the element edges. (C) Top and side views of the deformed FE mesh after specifying a uniform in situ fiber strain of 3% using Eq. (1). Fringe values are fiber strain. Legend applies to panels C–F. Note that the fiber strain is highly inhomogeneous and values at every location are lower than the desired value of 3%. (D) Fringe plots of fiber strain on deformed FE mesh after one iterative update using Eq. (6). (E) Fringe plots of fiber strain after two iterative updates. (F) Fringe plots of fiber strain after five iterative updates. The fiber strain is completely uniform and has achieved a value of 3%.

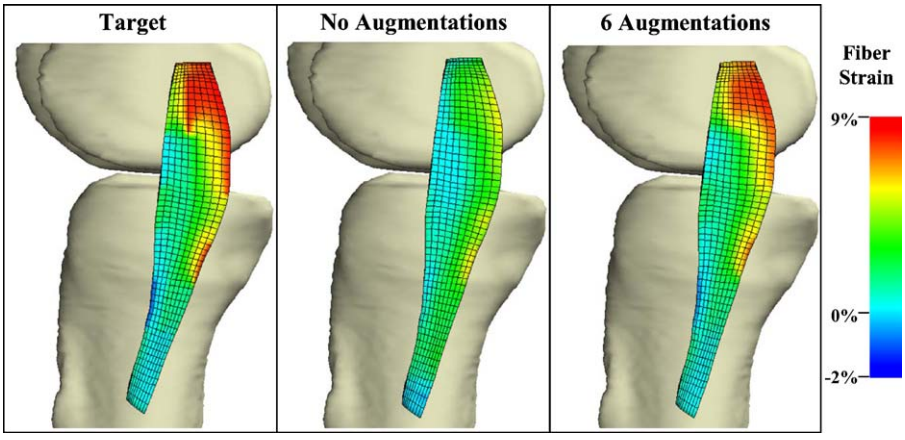

Fig. 7. Augmented Lagrangian enforcement of an experimental in situ strain distribution on an FE model of the human femur–medial collateral ligament (MCL)–tibia complex. Left panel-experimentally measured in situ strain distribution at 0 degrees of knee flexion. Middle panel-result after applying the in situ strain distribution to the MCL using Eq. (1) with no augmentations. The total in situ fiber strain ($\lambda_{0\rightarrow r}-1$) is much lower and less inhomogeneous than the target in situ strain distribution (compare left and middle panels). Right panel-results after six augmentations using the augmented Lagrangian algorithm. The resulting in situ strain distribution is nearly identical to the experimental distribution (compare left and right panels). The small differences between these two images are the result of using nodal values for the interpolation in the left panel and enforcing the constraint at the integration points in the right panel.

different ligaments, population-average values of in situ strain can be used in patient-specific FE models. However, this approach can only provide population-average predictions of strain under subsequent externally applied loads, as FE predictions of stress/strain are highly sensitive to the in situ strain distributions [7]. To circumvent this difficulty, a population-average in situ strain distribution could be scaled to an individual patient based on patient-specific measurements of initial joint laxity (assuming that a correlation could first be established in vitro).

6. Verification and validation

The phrase "verification and validation" has become popular in the recent literature on computational mechanics (see e.g [139,140]). In the context of the present paper, verification refers to the process of determining whether or not an FE model of a ligament can be used to represent the underlying principles of continuum mechanics with sufficient accuracy. Verification has two parts: (1) testing the ability of constitutive models, element technology, contact algorithms, etc. in an FE program to reproduce known analytical solutions to idealized problems within some well defined error tolerance, and (2) a posteriori error estimates, such as mesh convergence studies. Validation refers to comparison of FE model predictions with experimental measurements. It should be noted that there is no way to completely verify or validate an FE model of ligament mechanics. This is analogous to the way that scientific theories cannot be proven but only dis-proven [141]. However, once an exception is found, it invalidates that particular prediction or set of predictions under the conditions that were investigated. The investigator must pose specific hypotheses regarding model verification and validation, along with appropriately chosen tolerances, and then test these hypotheses. Repeated rejection of the null hypothesis (that the model does not reproduce the underlying principles of mechanics or that the model does not predict experimental data) for tests of the model's descriptive and predictive capabilities provides confidence in the use of the model for decision making.

6.1. Verification

Verification includes the assurance that constitutive models give the correct predictions for simple loading cases, that specific types of finite elements can reproduce desired modes of deformation (e.g., bending, shear) and that the FE mesh used to discretize the domain is of sufficient spatial resolution to provide the desired degree of accuracy. These assurances may be made by investigating both idealized problems/geometries and by working with the actual geometry of the FE model. In the case of the constitutive model, one must verify that the numerical implementation can reproduce various analytical solutions, such as for uniaxial, biaxial and shear loading. To verify that a particular type of finite element is capable of describing a particular type of deformation, an investigator may study simple problems of shear and bending, and compare predictions to analytical solutions. Finally, the spatial discretization error inherent in the FE method is assessed by performing mesh convergence studies. Since all FE structural models produce a solution that is "too stiff" when compared to known solutions and can only reproduce the exact analytical solution as elements become infinitely small, the assessment of overall model stiffness is typically investigated as a function of mesh density. By performing numerous solutions of a similar problem with different mesh resolutions, the investigator can determine the mesh resolution that provides sufficient accuracy for the needs of the study at hand. All aspects of the verification process should be performed before any model validation tests are pursued.

6.2. Validation

The comparison of model predictions to experimental measurements constitutes the validation process. As mentioned above, there is no way to completely validate a model. One must pose specific hypotheses about model predictions along with tolerable errors. Validation is the most challenging aspect of the FE modeling of ligament mechanics, as it requires accurate experimental measurements of quantities that are difficult to measure. Further, the computational biomechanist is often inappropriately trained or ill-equipped to perform the necessary experiments. An appropriate collaborator is critical in this situation, as the use of experimental data in the literature for validation can present a number of problems.

FE models of ligament mechanics are typically designed with the hope of predicting stress and strain distributions, insertion site forces and contact forces as ligaments wrap around bones and other ligaments. These quantities are often used for model validation [7,23]. It is inappropriate to rely solely on yes/no hypotheses for comparison of FE predictions with experimental data. Acceptance of the null hypothesis that model predictions are "not significantly different" from experimental measurements does not provide a good means to perform model validation, since this conclusion says nothing by itself of statistical power or the amount of variation in the experimental data that may be explained by the model. Regression analyses provide a convenient way to assess the correlation between FE predictions and experimental measurements [7]. When interpreting any type of statistical results regarding FE model validation, one must consider the magnitude of errors that are associated with the experimental measurements.

Experimental measurements of insertion site reaction forces, global joint kinematics and ligament strains have been used in the validation process for FE models of ligaments [7,12,23,25,142]. Insertion site forces and global joint kinematics can be measured in an experimental setting using one of several different methods [31,143,144]. These are "global"

or "integrated" measurements in terms of model validation, since numerous assumptions associated with the FE model contribute to the accuracy of such a prediction. The inability of an FE ligament model to predict insertion site forces or joint kinematics within some pre-defined error band indicates a problem somewhere, but does not localize the problem to the constitutive model, mesh, or boundary conditions. However, the ability of an FE ligament model to predict insertion site forces or joint kinematics does not provide validation of its ability to predict local ligament stresses and strains. The latter quantities indicate the potential for local tissue injury and remodeling, which are often of more interest to the analyst. A combined approach, including measurement of joint kinematics, insertion site forces and local ligament strains, provides a framework for the most thorough validation of FE models of ligament mechanics. When assessing agreement between experimental measurements and computational predictions, it is important to quantify the errors associated with the experimental measurements. For instance, in the measurement of ligament strain, errors are the result of the inherent accuracy/precision of the measurement method [145] as well as any uncertainty in defining the reference (stress-free) configuration.

6.3. Sensitivity studies

Inputs to an FE model, whether measured experimentally or obtained from the literature, should not be assumed to be absolute known quantities. As an example, consider material coefficients for a constitutive model. These material coefficients may be based on subject-specific measurements or on population averages. In the former case, there is uncertainty in these coefficients due to the inherent errors in experimental measurements. In the latter case, the coefficients represent a population average, and thus, have some well-defined variance. In both cases, it is desirable to characterize the sensitivity of FE model predictions to variations in the material coefficients. The magnitude of the variations may be chosen, based on the standard deviations of the population or based on knowledge of the errors associated with the experimental measurements. This is even more important in the common case of model input parameters for which experimental data are not available. In this situation, the parameters should be varied over a wide range, based on the analyst's assessment of physically reasonable/admissible values. This type of sensitivity study (or parameter study) can yield important insight into the physics of the model, and thus, improve confidence in model predictions. Sensitivity studies should be performed for both experimentally measured and "assumed" model inputs.

7. Discussion and future directions

The objective of this paper was to describe techniques that can facilitate the construction, analysis and validation of FE models of ligaments. The authors hope that this information will assist other investigators in their research and provide guidelines for the development and critical assessment of ligament FE models. The methodologies described in this work can be readily adapted to the study of many different ligamentous structures and joints. This should provide a solid foundation for further studies of ligament injury, healing, and patient-specific clinical treatment. There are a number of areas where further research is desperately needed to advance the state of the art, and these are discussed individually below.

The development and validation of whole-joint models that include three-dimensional ligament geometries is an area where further research is needed. The difficulty with validation of these models is that models of individual ligaments must be validated separately. Without such an approach, it is impossible to determine the predictive capability of these models beyond prediction of overall joint kinematics. Although the literature contains many examples of whole-joint models, few use three-dimensional representations for the ligaments and none have been validated using the approaches described in Section 6 above.

The construction of three-dimensional FE models of ligaments can be extremely time consuming due to the need to acquire three-dimensional geometry from medical image data, segment the ligaments and bones of interest, and generate FE meshes. This process is especially difficult for image data obtained in vivo, since the boundaries of soft tissues in MR and CT images are difficult to discern. Improvements in MR imaging sequences for ligaments are needed to provide better contrast and signal. This alone will greatly facilitate the extraction of three-dimensional geometric information from images acquired in vivo. Although tools for segmentation are quite mature and effective, similar tools for mesh generation remain difficult to use and cannot provide automatically generated meshes that can yield accurate FE solutions.

There are a number of areas related to constitutive models for ligaments that will benefit from further research and development. One goal of the analysis of ligament mechanics is to assess the propensity for injury under various externally applied loading conditions. This requires suitable criteria for material failure, and data in the literature on the material failure of ligaments is entirely based on uniaxial testing along the predominant fiber direction. Additional experimental data are needed to develop multiaxial material failure theories for these anisotropic materials. Further improvements in constitutive models may be made by a better understanding of the contribution of the "ground substance" to continuum level material properties. The exact mechanisms by which proteoglycans influence ligament material properties remain to be determined. Finally, the role of fluid flow in ligament material behavior is still poorly understood. Data on the permeability of ligament, along and transverse to the fiber direction, will help to clarify these effects.

The representation of ligament insertions to bone in FE models must be refined to better represent stress transfer, and thus provide improved predictions of the potential for failure at the insertion sites. Ligament insertion sites reduce the stress concentrations that naturally occur as forces are transferred across the ligament–bone interface. The junction between the soft tissue of ligaments and the hard tissue of bones is complex and can vary greatly between ligaments as well as between the two ends of the same ligament. Ligament insertion sites have been broadly categorized into two categories, direct and indirect. Direct insertion sites are generally well-defined areas with a sharp boundary between the bone and the attaching ligament occurring over a distance of less than 1 mm [84]. The collagen fibrils quickly pass out of normal ground substance matrix and continue through zones of fibrocartilage, mineralized fibrocartilage, and finally into bone [146]. Most of the fibrils at direct insertion sites are deep fibrils that meet the bone at approximately right angles. Indirect insertion sites attach to the bone over a broader area than direct insertion sites and have a more gradual transition between hard and soft tissue. The superficial fibers dominate at indirect sites and their attachment to bone occurs mainly through fibers blending with the periosteum. The deep fibers of indirect insertions have been shown to attach directly to bone at acute angles without the fibrocartilagenous transitional zone observed in direct insertions [147]. Despite the gradual change from soft to hard tissue, insertion sites are often the location of injuries. This is especially true when rapid remodeling of the insertion sites takes place during skeletal maturation or after joint immobilization [148–151]. Tissue strains near the insertion sites have been shown to differ from strains measured in the midsubstance of ligaments [68,152]. Material inhomogeneities are believed to be especially common near the insertion sites [153], although this has not been well quantified experimentally due to the difficulties in performing mechanical measurements in such a small region of tissue.

Although it is clear that accurate representation of ligament in situ strain is critical to accurate predictions of ligament stresses, strains and insertion site forces [25,132], data on ligament in situ strains are extremely limited. This is especially important if subject-specific modeling techniques are ever to be applied in the clinic for treatment planning or diagnostics. Future research should focus on establishing relationships between joint laxity in vivo and in situ ligament strains, as these data would provide the means to apply subject-specific modeling techniques to the study of the joints of individual patients.

Finally, the authors strongly encourage other investigators to adopt a systematic approach to model verification and validation. This is often not given the attention that it merits. The long-term success of FE modeling in experimental studies and clinical application, as well as the success of the FE method in other areas of biomechanics, hinges on the proper verification and validation of computational models.

Acknowledgments

Financial support from NIH grants #AR47369 and #AR050218 is gratefully acknowledged. The authors thank their collaborators at the University of Pittsburgh, Dr. Richard Debski and Ms. Susan Moore, for providing the CT data of the inferior glenohumeral ligament, Drs. Dennis Parker and S.-E. Kim of the Department of Radiology at the University of Utah for implementing the MR acquisition sequences that were used for short T2 imaging of ligaments, and Dr. David Weinstein of the Scientific Computing and Imaging Institute at the University of Utah for assistance with volume rendering using the SCIRun software.

References

[2] Atkinson TS, Haut RC, Altiero NJ. A poroelastic model that predicts some phenomological responses of ligaments and tendons. J Biomech Eng 1997;119:400–5.
[3] Bendjaballah MZ, Shirazi-Adl A, Zukor DJ. Finite element analysis of human knee joint in varus-valgus. Clin Biomech (Bristol Avon) 1997;12:139–48.
[4] Gardiner JC, Weiss JA, Experimental testing and computational modeling to determine the stress–strain distribution in the human medial collateral ligament. Presented at 44th Annual Meeting Orthopaedic Research Society, New Orleans, LA; 1998.
[5] Heegaard J, Leyvraz PF, Curnier A, Rakotomanana L, Huiskes R. The biomechanics of the human patella during passive knee flexion. J Biomech 1995;28:1265–79.
[6] Hirokawa S, Tsuruno R. Three-dimensional deformation and stress distribution in an analytical/computational model of the anterior cruciate ligament. J Biomech 2000;33:1069–77.
[7] Gardiner JC, Weiss JA. Subject-specific finite element analysis of the human medial collateral ligament during valgus knee loading. J Orthop Res 2003;21:1098–106.
[8] Grood ES, Hefzy MS. An analytical technique for modeling knee joint stiffness—part I: ligamentous forces. J Biomech Eng 1982;104:330–7.
[9] Mommersteeg TJ, Huiskes R, Blankevoort L, Kooloos JG, Kauer JM, Maathuis PG. A global verification study of quasi-static knee model with multi-bundle ligaments. J Biomech 1996;29:1659–64.
[10] Wismans J, Veldpaus F, Janssen J, Huson A, Struben P. A three-dimensional mathematical model of the knee-joint. J Biomech 1980;13:677–85.
[11] Blankevoort L, Huiskes R. Ligament–bone interaction in a three-dimensional model of the knee. J Biomech Eng 1991;113:263–9.
[12] Li G, Kanamori A, Woo SL-Y. A validated three-dimensional computational model of a human knee joint. J Biomech Eng 1999;121:657–62.
[13] Giori NJ, Beaupre GS, Carter DR. Cellular shape and pressure may mediate mechanical control of tissue composition in tendons. J Orthop Res 1993;11:581–91.
[14] Matyas JR, Anton MG, Shrive NG, Frank CB. Stress governs tissue phenotype at the femoral insertion of the rabbit MCL. J Biomech 1995;28:147–57.
[15] Arms S, Boyle J, Johnson R, Pope M. Strain measurement in the medial collateral ligament of the human knee: an autopsy study. J Biomech 1983;16:491–6.
[16] Berns GS, Hull ML, Patterson HA. Strain in the anteromedial bundle of the anterior cruciate ligament under combination loading. J Orthop Res 1992;10:167–76.

[17] Gardiner JC, Weiss JA, Rosenberg TD. Strain in the human medial collateral ligament during valgus loading of the knee. Clin Orthop 2001;391:266–74.
[18] Hull ML, Berns GS, Varma H, Patterson HA. Strain in the medial collateral ligament of the human knee under single and combined loads. J Biomech 1996;29:199–206.
[19] Woo SL-Y, Weiss JA, Gomez MA, Hawkins DA. Measurement of changes in ligament tension with knee motion and skeletal maturation. J Biomech Eng 1990;112:46–51.
[20] Kawada T, Abe T, Yamamoto K, Hirokawa S, Soejima T, Tanaka N, et al. Analysis of strain distribution in the medial collateral ligament using a photoelastic coating method. Med Eng Phys 1999;21:279–91.
[21] Bandak FA, Tannous RE, Toridis T. On the development of an osseo-ligamentous finite element model of the human ankle joint. Inter J Solids Structures 2001;38:1681–97.
[22] Penrose JM, Holt GM, Beaugonin M, Hose DR. Development of an accurate three-dimensional finite element knee model. Comput Meth Biomech Biomed Eng 2002;5:291–300.
[23] Song Y, Debski RE, Musahl V, Thomas M, Woo SL. A three-dimensional finite element model of the human anterior cruciate ligament: a computational analysis with experimental validation. J Biomech 2004;37:383–90.
[24] Debski RE, Weiss JA, Newman WJ, Moore SM, McMahon PJ. Stress and strain in the anterior band of the inferior glenohumeral ligament during a simulated clinical exam. J Shoulder Elbow Surg 2005;14:24S–31S.
[25] Limbert G, Taylor M, Middleton J. Three-dimensional finite element modelling of the human ACL: simulation of passive knee flexion with a stressed and stress-free ACL. J Biomech 2004;37:1723–31.
[26] Li G, Gil J, Kanamori A, Woo SL. A validated three-dimensional computational model of a human knee joint. J Biomech Eng 1999;121:657–62.
[27] Reichert IL, Benjamin M, Gatehouse PD, Chappell KE, Holmes J, He T, et al. Magnetic resonance imaging of periosteum with ultrashort TE pulse sequences. J Magn Reson Imaging 2004;19:99–107.
[28] Gold GE, Pauly JM, Macovski A, Herfkens RJ. MR spectroscopic imaging of collagen: tendons and knee menisci. Magn Reson Med 1995;34:647–54.
[29] Kim SE, Phatak N, Buswell H, Jeong EK, Weiss JA, Parker DL. Short TE double echo 3D SPGR acquistion for short T2 imaging. In: Presented at Proceedings of the 11th Scientific Meeting of International Society for Magnetic Resonance in Medicine. 2003.
[30] Fischer KJ, Manson TT, Pfaeffle HJ, Tomaino MM, Woo SL-Y. A method for measuring joint kinematics designed for accurate registration of kinematic data to models constructed from CT data. J Biomech 2001;34:377–83.
[31] Lujan TJ, Lake SP, Plaizier TA, Ellis BJ, Weiss JA. Simultaneous measurement of three-dimensional joint kinematics and tissue strains with optical methods. ASME J Biomech Eng 2005;127:193–7.
[32] Limbert G, Middleton J, Taylor M. Finite element analysis of the human ACL subjected to passive anterior tibial loads. Comput Meth Biomech Biomed Eng 2004;7:1–8.
[33] Simbeya KW, Shrive NG, Frank CB, Matyas JR. A micromechanical finite element model of the rabbit medial collateral ligament. In: Middleton J, Pande G, Williams K, editors. Recent advances in computer methods in biomechanics and biomedical engineering. Books and Journals Ltd.; 1992.
[34] Boissonnat JD. Shape reconstruction from planar cross-sections, Computer Vision. Graphics Image Process 1988;44:1–29.
[35] Lorensen WE, Cline HE. Marching cubes: a high resolution 3D surface construction algorithm. Comp Graph (Proc SIGGRAPH) 1987;4:163–9.
[36] Schroeder WJ, Zarge J, Lorensen WE. Decimation of triangle meshes. Comp Graph (Proc SIGGRAPH) 1992;25.
[37] Maker BN, Rigid bodies for metal forming analysis with NIKE3D. University of California, Lawrence Livermore Lab Rept 1995;UCRL-JC-119862:1–8.
[38] Taylor RL. Mixed-enhanced formulation for tetrahedral finite elements. Inter J Numerical Meth Eng 2000;47:205–27.
[39] Beissel SR, Johnson GR. Large-deformation triangular and tetrahedral element formulations for unstructured meshes. Comput Meth Appl Mech Eng 2000;187:469–82.
[40] Hughes TJR, Liu WK. Nonlinear finite element analysis of shells-1. Three-dimensional shells. Comput Meth Appl Mech Eng 1981;26:331–62.
[41] Hughes TJR, Carnoy E. Nonlinear finite element shell formulation accounting for large membrane strains. Proc ASME Winter Annual Meeting 1981;48:193–208.
[42] Newman WJ, Debski RE, Moore SM, Weiss JA, Development of a finite element model of the inferior glenohumeral ligament of the glenohumeral joint. In: Proceedings of the ASME International Mechanical Engineering Congress & Exposition 2003;IMECE2003-43137.
[43] Moore SM, McMahon PJ, Debski RE. Bi-directional mechanical properties of the axillary pouch of the glenohumeral capsule: implications for modeling and surgical repair. J Biomech Eng 2004;126:284–8.
[44] Quapp KM, Weiss JA. Material characterization of human medial collateral ligament. J Biomech Eng 1998;120:757–63.
[45] Stabile KJ, Pfaeffle J, Weiss JA, Fischer K, Tomaino MM. Bi-directional mechanical properties of the human forearm interosseous ligament. J Orthop Res 2004;22:607–12.
[46] Debski RE, Moore SM, Mercer JL, Sacks MS, McMahon PJ. The collagen fibers of the anteroinferior capsulolabrum have multiaxial orientation to resist shoulder dislocation. J Shoulder Elbow Surg 2003;12:247–52.
[47] Butler DL, Guan Y, Kay MD, Cummings JF, Feder SM, Levy MS. Location-dependent variations in the material properties of the anterior cruciate ligament. J Biomech 1992;25:511–8.
[48] Comninou M, Yannas IV. Dependence of stress–strain nonlinearity of connective tissues on the geometry of collagen fibers. J Biomech 1976;9:427–33.
[49] Diamant J, Keller A, Baer E, Litt M, Arridge RGC. Collagen; ultrastructure and its relation to mechanical properties as a function of ageing. Proc R Soc London, Ser B Biol Sci 1972;180:293–315.
[50] Hansen KA, Weiss JA, Barton JK, Recruitment of tendon crimp with applied tensile strain, ASME J Biomech Eng, 2002, in press.
[51] Woo SL-Y. Mechanical properties of tendons and ligaments. I. Quasi-static and nonlinear viscoelastic properties. Biorheology 1982;19:385–96.
[52] Woo SL-Y, Ohland KJ, Weiss JA. Aging and sex-related changes in the biomechanical properties of the rabbit medial collateral ligament. Mech Ageing Dev 1990;56:129–42.
[53] Viidik A, Ekholm R. Light and electron microscopic studies of collagen fibers under strain. Z Anat Entwickl Gesch 1968;127:154–64.
[54] Frisen M, Magi M, Sonnerup L, Viidik A. Rheological analysis of soft collagenous tissue. Part I: Theoretical considerations. J Biomech 1969;2:13–20.
[55] Frisen M, Magi M, Sonnerup L, Viidik A. Rheological analysis of soft collagenous tissue. Part II: Experimental evaluations and verifications. J Biomech 1969;2:21–8.
[56] Kastelic J, Palley I, Baer E. A structural mechanical model for tendon crimping. J Biomech 1980;13:887–93.
[57] Lanir Y. A structural theory for the homogeneous biaxial stress–strain relationships in flat collagenous tissues. J Biomech 1979;12:423–36.
[58] Decraemer WF, Maes MA, Vanhuyse VJ. An elastic stress–strain relation for soft biological tissues based on a structural model. J Biomech 1980;13:463–8.
[59] Belkoff SM, Haut RC. Microstructurally based model analysis of gamma-irradiated tendon allografts. J Orthop Res 1992;10:461–4.

[60] Kwan MK, Woo SL-Y. A structural model to describe the nonlinear stress–strain behavior for parallel-fibered collagenous tissues. J Biomech Eng 1989;111:361–3.
[61] Soong YT, Huang WN. A stochastic model for biological tissue elasticity in simple elongation. J Biomech 1973;6:451–8.
[62] Lanir Y. Structure-function relations in mammalian tendon: the effect of geometrical nonuniformity. J Bioeng 1978;2:119–28.
[63] Liao H, Belkoff SM. A failure model for ligaments. J Biomech 1999;32:183–8.
[64] Lanir Y. Constitutive equations forfibrous connective tissues. J Biomech 1983;16:1–12.
[65] Stouffer DC, Butler DL, Hosny D. The relationship between crimp pattern and mechanical response of human patellar tendon-bone units. J Biomech Eng 1985;107:158–65.
[66] Kwan MK, Lin TH, Woo SL-Y. On the viscoelastic properties of the anteromedial bundle of the anterior cruciate ligament. J Biomech 1993;26:447–52.
[67] Woo SL-Y, Gomez MA, Akeson WH. The time and history-dependent viscoelastic properties of the canine medial collateral ligament. J Biomech Eng 1981;103:293–8.
[68] Woo SL-Y, Gomez MA, Seguchi Y, Endo CM, Akeson WH. Measurement of mechanical properties of ligament substance from a bone–ligament–bone preparation. J Ortho Res 1983;1:22–9.
[69] Chimich D, Shrive N, Frank C, Marchuk L, Bray R. Water content alters viscoelastic behavior of the normal adolescent rabbit medial collateral ligament. J Biomech 1992;25:831–7.
[70] Cohen RE, Hooley CJ, McCrum NG. Viscoelastic creep in collagenous tissue. J Biomech 1976;9:175–84.
[71] Lam TC, Thomas CG, Shrive NG, Frank CB, Sabiston CP. The effects of temperature on the viscoelastic properties of the rabbit medial collateral ligament. J Biomech Eng 1990;112:147–52.
[72] Pioletti DP, Heegaard JH, Rakotomanana RL, Leyvraz PF, Blankevoort L. Experimental and mathematical methods for representing relative surface elongation of the ACL. J Biomech 1995;28:1123–6.
[73] Yahia LH, Audet J, Drouin G. Rheological properties of the human lumbar spine ligaments. J Biomed Eng 1991;13:399–406.
[74] Bonifasi-Lista C, Lake SP, Small MS, Weiss JA. Viscoelastic properties of the human medial collateral ligament under longitudinal, transverse and shear loading. J Orthop Res 2005;23:67–76.
[75] Woo SL-Y, Peterson RH, Ohland KJ, Sites TJ, Danto MI. The effects of strain rate on the properties of the medial collateral ligament in skeletally immature and mature rabbits: a biomechanical and histological study. J Ortho Res 1990;8:712–21.
[76] Thielke RJ, Vanderby R, Grood ES, Volumetric changes in ligaments under tension, Presented at ASME Summer Bioengineering Conference, Beaver Creek, CO; 1995.
[77] Weiss JA, Maakestad B, Permeability of human medial collateral ligament in compression transverse to the collagen fiber direction. J Biomech 2005; in press.
[78] Hannafin JA, Arnoczky SP. Effect of cyclic and static tensile loading on water content and solute diffusion in canine flexor tendons: an in vitro study. J Ortho Res 1994;12:350–6.
[79] Butler DL, Kohles SS, Thielke RJ, Chen C, Vanderby R. Interstitial fluid flow in tendons and ligaments: a porous medium finite element solution. Med Biol Eng Comput 1997;35:742–6.
[80] Chen CT, Malkus DS, Vanderby R. A fiber matrix model for interstitial fluid flow and permeability in ligaments and tendons. Biorheology 1998;35:103–18.
[81] Weiss J, Maakestad B, Nisbet J, The permeability of human medial collateral ligament, Presented at 46th Annual Meeting of the Orthopaedic Research Society, Orlando, FL; 2000.
[82] Daniel DM, Akeson WH, O'Connor JJ. Knee ligaments: structure, function, injury and repair. New York: Raven Press; 1990.
[83] Amiel D, Frank C, Harwood F, Fronek J, Akeson W. Tendons and ligaments: a morphological and biochemical comparison. J Ortho Res 1984;1:257–65.
[84] Woo SL-Y, Buckwalter JA. Injury and repair of the musculoskeletal soft tissues. Park Ridge, Illinois: American Academy of Orthopaedic Surgeons; 1988.
[85] Plaas AH, Wong-Palms S, Koob T, Hernandez D, Marchuk L, Frank CB. Proteoglycan metabolism during repair of the ruptured medial collateral ligament in skeletally mature rabbits. Arch Biochem Biophys 2000;374:35–41.
[86] Waggett AD, Ralphs JR, Kwan AP, Woodnutt D, Benjamin M. Characterization of collagens and proteoglycans at the insertion of the human Achilles tendon. Matrix Biol 1998;16:457–70.
[87] Scott JE. How rational histochemistry produced order out of chaos in the "amorphous ground substance" (with a little help from biochemistry, biophysics etc.). Eur J Histochem 1998;42(Spec No):29–34.
[88] Scott JE. Alcian blue. Now you see it, now you don't. Eur J Oral Sci 1996;104:2–9.
[89] Scott JE, Orford CR. Dermatan sulphate-rich proteoglycan associates with rat tail-tendon collagen at the d band in the gap region. Biochem J 1981;197:213–6.
[90] Pogany G, Hernandez DJ, Vogel KG. The in vitro interaction of proteoglycans with type I collagen is modulated by phosphate. Arch Biochem Biophys 1994;313:102–11.
[91] Svensson L, Heinegard D, Oldberg A. Decorin-binding sites for collagen type I are mainly located in leucine-rich repeats 4–5. J Biol Chem 1995;270:20712–6.
[92] Pringle GA, Dodd CM. Immunoelectron microscopic localization of the core protein of decorin near the d and e bands of tendon collagen fibrils by use of monoclonal antibodies. J Histochem Cytochem 1990;38:1405–11.
[93] Sorrell JM, Carrino DA, Baber MA, Asselineau D, Caplan AI. A monoclonal antibody which recognizes a glycosaminoglycan epitope in both dermatan sulfate and chondroitin sulfate proteoglycans of human skin. Histochem J 1999;31:549–58.
[94] Elliott DM, Robinson PS, Gimbel JA, Sarver JJ, Abboud JA, Iozzo RV, et al. Effect of altered matrix proteins on quasilinear viscoelastic properties in transgenic mouse tail tendons. Ann Biomed Eng 2003;31:599–605.
[95] Ameye L, Young MF. Mice deficient in small leucine-rich proteoglycans: novel in vivo models for osteoporosis, osteoarthritis, Ehlers–Danlos syndrome, muscular dystrophy, and corneal diseases. Glycobiology 2002;12:107R–16R.
[96] Corsi A, Xu T, Chen XD, Boyde A, Liang J, Mankani M, et al. Phenotypic effects of biglycan deficiency are linked to collagen fibril abnormalities, are synergized by decorin deficiency, and mimic Ehlers–Danlos-like changes in bone and other connective tissues. J Bone Miner Res 2002;17:1180–9.
[97] Danielson KG, Baribault H, Holmes DF, Graham H, Kadler KE, Iozzo RV. Targeted disruption of decorin leads to abnormal collagen fibril morphology and skin fragility. J Cell Biol 1997;136:729–43.
[98] Hakkinen L, Strassburger S, Kahari VM, Scott PG, Eichstetter I, Lozzo RV, et al. A role for decorin in the structural organization of periodontal ligament. Lab Invest 2000;80:1869–80.
[99] Reed CC, Iozzo RV. The role of decorin in collagen fibrillogenesis and skin homeostasis. Glycoconj J 2002;19:249–55.
[100] Graham HK, Holmes DF, Watson RB, Kadler KE. Identification of collagen fibril fusion during vertebrate tendon morphogenesis. The process relies on unipolar fibrils and is regulated by collagen–proteoglycan interaction. J Mol Biol 2000;295:891–902.
[101] Caprise PA, Lester GE, Weinhold P, Hill J, Dahners LE. The effect of NKISK on tendon in an in vivo model. J Orthop Res 2001;19:858–61.
[102] Beskos DE, Jenkins JT. A mechanical model for mammalian tendon. J Appl Math 1975;42:755–8.
[103] Ault HK, Hoffman AH. A composite micromechanical model for connective tissues: Part I Theory. J Biomech Eng 1992;114:137–41.

[104] Ault HK, Hoffman AH. A composite micromechanical model for connective tissues: Part II Application to rat tail tendon and joint capsule. J Biomech Eng 1992;114:142–6.
[105] Hurschler C, Loit-Ramage B, Vanderby R. A structurally based stress–stretch relationship for tendon and ligament. J Biomech Eng 1997;119:392–9.
[106] Gardiner JC, Weiss JA. Simple shear testing of parallel-fibered planar soft tissues. J Biomech Eng 2001;123:170–5.
[107] Weiss JA, Maker BN, Govindjee S. Finite element implementation of incompressible, transversely isotropic hyperelasticity. Comp Meth Appl Mech Eng 1996;135:107–28.
[108] Weiss JA, Gardiner JC, Bonifasi-Lista C. Ligament material behavior is nonlinear, viscoelastic and rate-independent under shear loading. J Biomech 2002;35:943–50.
[109] Fung YC. Biomechanics: mechanical properties of living tissues. New York: Springer-Verlag; 1993.
[110] Danto MI, Woo SL-Y. The mechanical properties of skeletally mature rabbit anterior cruciate ligament and patellar tendon over a range of strain rates. J Ortho Res 1993;11:58–67.
[111] Yahia LH, Drouin G. Study of the hysteresis phenomenon in canine anterior cruciate ligaments. J Biomed Eng 1990;12:57–62.
[112] Thornton GM, Oliynyk A, Frank CB, Shrive NG. Ligament creep cannot be predicted from stress relaxation at low stresses: a biomechanical study of the rabbit medial collateral ligament. J Ortho Res 1997;15:652–6.
[113] Panjabi MM, Courtney TW. High-speed subfailure stretch of rabbit anterior cruciate ligament: changes in elastic, failure and viscoelastic characteristics. Clin Biomech (Bristol Avon) 2001;16:334–40.
[114] Bray RC, Doschak MR, Gross TS, Zernicke RF. Physiological and mechanical adaptations of rabbit medial collateral ligament after anterior cruciate ligament transection. J Orthop Res 1997;15:830–6.
[115] Rupp S, Seil R, Kohn D, Muller B. The influence of avascularity on the mechanical properties of human bone–patellar–tendon–bone grafts. J Bone Joint Surg Br 2000;82:1059–64.
[116] Panjabi MM, Moy P, Oxland TR, Cholewicki J. Subfailure injury affects the relaxation behavior of rabbit ACL. Clin Biomech (Bristol Avon) 1999;14:24–31.
[117] Abramowitch SD, Woo SL, Clineff TD, Debski RE. An evaluation of the quasi-linear viscoelastic properties of the healing medial collateral ligament in a goat model. Ann Biomed Eng 2004;32:329–35.
[118] Lanir Y. A micro structure model for the rheology of mammalian tendon. J Biomech Eng 1980;102:332–9.
[119] Lanir Y. Constitutive equations for fibrous connective tissues. J Biomech 1983;16:1–12.
[120] Decraemer WF, Maes MA, Vanhuyse VJ, Vanpeperstraete P. A nonlinear viscoelastic constitutive equation for soft biological tissues, based upon a structural model. J Biomech 1980;13:559–64.
[121] Sanjeevi R, Somanathan N, Ramaswamy D. A viscoelastic model for collagen fibres. J Biomech 1982;15:181–3.
[122] Sanjeevi R. A viscoelastic model for the mechanical properties of biological materials. J Biomech 1982;15:107–9.
[123] Dehoff PH. On the nonlinear viscoelastic behavior of soft biological tissues. J Biomech 1978;11:35–40.
[124] Bingham DN, Dehoff PH. A constitutive equation for the canine anterior cruciate ligament. J Biomech Eng 1979;101:15–22.
[125] Johnson GA, Livesay GA, Woo SL, Rajagopal KR. A single integral finite strain viscoelastic model of ligaments and tendons. J Biomech Eng 1996;118:221–6.
[126] Pioletti DP, Rakotomanana LR, Benvenuti JF, Leyvraz PF. Viscoelastic constitutive law in large deformations: application to human knee ligaments and tendons. J Biomech 1998;31:753–7.
[127] Quaglini V, Vena P, Contro R. A discrete-time approach to the formulation of constitutive models for viscoelastic soft tissues. Biomech Model Mechanobiol 2004.
[128] Bischoff JE, Arruda EM, Grosh K. A rheological network model for the continuum anisotropic and viscoelastic behavior of soft tissue. Biomech Model Mechanobiol 2004;3:56.
[129] Bonifasi-Lista C, Lake SP, Small MS, Weiss JA. Viscoelastic properties of the human medial collateral ligament under longitudinal, transverse and shear loading. J Orthop Res 2005;23:67–76.
[130] Pioletti DP, Rakotomanana L, Gillieron C, Leyvraz PF, Benvenuti JF, Nonlinear viscoelasticity of the ACL: experiments and theory. In: Middleton JaJ, ML, Pande, GN (Eds.) Comp Meth Biomech Biomed Eng. 1996.
[131] Puso MA, Weiss JA. Finite element implementation of anisotropic quasilinear viscoelasticity. J Biomech Eng 1998;120:62–70.
[132] Gardiner JC, Weiss JA, Rosenberg TD. Strain in the human medial collateral ligament during valgus loading of the knee. Clin Orthop 2001:266–74.
[133] Weiss JA, Maker BN, Schauer DA, Treatment of initial stress in hyperelastic finite element models of soft tissues. ASME Summer Bioengineering Conference 1995;BED-29:105–6.
[134] Fletcher R. Practical methods of optimization. New Delhi: Wiley and Sons; 1989.
[135] Fortin M, Glowinski R, Augmented lagrangian methods: applications to the numerical solution of boundary-value problems. 1983.
[136] Powell MJD. A method for nonlinear constraints in minimization problems. In: Fletcher R, editor. Optimization. New York: Academic Press; 1969.
[137] Hestenes MR. Multiplier and gradient methods. J Optim, Theory Applications 1969;4:303–20.
[138] Weiss JA, Schauer DA, Gardiner JC, Modeling contact in biological joints using penalty and augmented Lagrangian methods. ASME Winter Annual Meeting 1996;BED-33:347–348.
[139] Babuska I, Oden JT. Verification and validation in computational engineering and science: basic concepts. Comput Meth Appl Mech Eng 2004;193:4057–66.
[140] Roach PJ. Verification and validation in computational science and engineering. Socorro: Hermosa Publishers; 1998.
[141] Popper KR. The logic of scientific discovery. London: Routledge; 1992, originally published 1959 by Hutchinson Education.
[142] Li G, Suggs J, Gill T. The effect of anterior cruciate ligament injury on knee joint function under a simulated muscle load: a three-dimensional computational simulation. Ann Biomed Eng 2002;30:713–20.
[143] Debski RE, Wong EK, Woo SL, Sakane M, Fu FH, Warner JJ. In situ force distribution in the glenohumeral joint capsule during anterior-posterior loading. J Orthop Res 1999;17:769–76.
[144] Fujie H, Mabuchi K, Woo SL-Y, Livesay GA, Arai S, Tsukamoto Y. The use of robotics technology to study human joint kinematics: a new methodology. ASME J Biomech Eng 1993;115:211–7.
[145] Lujan TJ, Lake SP, Plaizier TA, Ellis BJ, Weiss JA. Simultaneous measurement of three-dimensional joint kinematics and ligament strains with optical methods. ASME J Biomech Eng 2005;127:193–7.
[146] Cooper RR, Misol S. Tendon and ligament insertion. a light and electron microscopic study. J Bone Joint Surg (Am) 1970;52:1–20.
[147] Benjamin M, Evans EJ, Copp L. The histology of tendon attachments to bone in man. J Anat 1986;149:89–100.
[148] Noyes FR, Torvik PJ, Hyde WB, LeLucas MS. Biomechanics of ligament failure. II. An analysis of immobilization, exercise and reconditioning effects in primates. J Bone Joint Surg (Am) 1974;56:1406–18.
[149] Tipton CM, Matthes RD, Martin RR. Influence of age and sex on the strength of bone-ligament junctions in knee joints of rats. J Bone Joint Surg (Am) 1978;60:230–4.

[150] Vailas AC, Tipton CM, Matthew RD, Gant M. Physical activity and its influence on the repair process of medial collateral ligaments. Connective Tissue Res 1981;9:25–31.

[151] Woo SL-Y, Gomez MA, Sites TJ, Newton PO, Orlando CA, Akeson WH. The biomechanical and morphological changes in the medial collateral ligament of the rabbit after immobilization and remobilisation. J Bone Joint Surg (Am) 1987;69:1200–11.

[152] Noyes FR, Butler DL, Grood ES, Zernicke RF, Hefzy MS. Biomechanical analysis of human ligament grafts used in knee-ligament repairs and reconstructions. J Bone Joint Surg (Am) 1984;66:344–52.

[153] Frank C, McDonald D, Lieber R, Sabiston P. Biochemical heterogeneity within the maturing rabbit medial collateral ligament. Clin Ortho Related Res 1988;236:279–85.